

Assessment Evapotranspiration Remotely Sensed Data: Case Study – SAKHA – Egypt

Naglaa Elbendary⁽¹⁾, Asharaf M. Almoustafa⁽²⁾, Sami A. Mohamed⁽²⁾, Sherin A Zahran⁽³⁾

¹. FAO Office Cairo (Corresponding Author, email: Naglaa.Elbandary@fao.org)

². Irrigation and Hydraulic Department, Faculty of Engineering, Ain Shams University, Egypt.

³. Environmental and Climate Change Research Institute, National Water Research Center, Egypt and High Institute of Engineering and Technologies Al Obour

Abstract:

Evapotranspiration is a combined process of evaporation, interception, and transpiration, and it is a crucial factor in the hydrological cycle. ET is the largest outgoing water flux from the Earth's surface and the most difficult hydrological flux to estimate or model, especially at regional or global scales. The present paper is looking for an assessment of the deviation of remotely sensed ET and actual in-situ measurements from energy balance tower across various ecological zones by considering two different remote sensing products including MOD16A2, and WaPOR V3. Each of the addressed remote sensing products has different theories and algorithms to estimate evapotranspiration and are produced with different spatial resolutions varying from 20 m in the case of WaPOR data to 500 meters in case of MODIS data. Remotely sensed data has been compared with ground measurement to identify associated accuracy and bias. Reference to in-situ data which has been collected from Sakha research station belongs to the Agriculture Research Center (ARC) under the Egyptian Ministry of Agriculture and Land Reclamation (MoALR). This paper compares Remote Sensing products and In Situ data and discusses how an integrated approach to using these products could help enhance Evapotranspiration (ET) accuracy for numerous climatic and ecological purposes. Data analysis shows that remote sensing models of higher resolution including the WaPOR V.3 product compare well with observed data. Eight statistical factors have been used to assess remotely sensed ET data reference to ET measurements including Coefficient of Determination, Correlation, Root Mean Square Error, Relative RMSE., Mean Bias Error, mm, PB (%), and Kling-Gupta Efficiency (KGE). WaPOR performs better Coefficient of Determination compared to MODIS16A2. All seasons of the study indicate that WaPOR has better correlation values than MODIS16A2, with the exception of Season 4 (Rice). The relative RMSE of WaPOR is significantly lower and establishes more reliable performance. Regarding WaPOR data, there is reduced MBE observed throughout the majority of the seasons with some of them close to zero implying very low bias. Smaller PB are noted on WaPOR which indicates that it captures seasonal patterns of evapotranspiration better. Efficiency values of WaPOR are higher than MODIS16A2 indicating better performance during all the seasons. KGE scores demonstrate that WaPOR generates comparatively higher values for all seasons

Keywords: actual evapotranspiration; remote sensing; energy balance; WaPOR database

Date of Submission: 15-12-2024

Date of acceptance: 31-12-2024

I. Introduction:

Evapotranspiration is a key player in the hydrological cycle as it represents approximately 62% of the total precipitation over land globally. It refers to the sum of water particles moving from the land surface to the atmosphere via evaporation and transpiration process.

ET is the dominant factor in water outflow through the turf, which constitutes the 'consumptive' use of water in agricultural and vegetated regions. Everyone agreed that ET should be measured spatially and temporally to support such water resources utilization and management that include: quantifying water use across the various land-cover types, water resources management, water planning for irrigation both at scheme and farm levels, crop

water productivity assessment, yield forecast through modeling and simulation, calculation of agricultural drought coefficients, water balance and accountancy in various hydrological systems at small and large scales. It also helps formulate strategies on how to mitigate the impacts of climate change. (FAO, 2023.)

ET depends highly on environmental and meteorological conditions and hence differs considerably with regions and ecosystems as shown in Figure 1. These variations are due to various interactive n – factors which include meteorological factors, soil and biological factors. Of all the meteorological factors that affect ET rates, temperature steps up the rates tremendously by enhancing the heat trapped by plants. Soil and plant surface water vaporization is favored by increased temperatures as put by (Dunxian She, et. al., 2017) , where temperature was identified to affect ET fluctuations in different habitats. Another important component is solar radiation since higher levels of this component meet the required heat for water evaporation and subsequently increase ET rates, as revealed by (S. Mohan, et. al., 1996). Similarly, indirectly, humidity exerts an inverse impact on the ET rates. As the RH increases, the VPD decreases and thus the rate of the ET process is inhibited, as pointed out by. (Ze-Xin Fan, et. al., 2013). Being an agent that transports moist air around evaporation surfaces, high wind speed also maintains a high vapor gradient that enhances the enhancement of ET.

Therefore, conditions of the soil and the land surface also affect ET. Soil moisture is of greater concern especially for rain fed and irrigated farming as it relates to the evaporative part of ET. In arid zones therefore, water becomes a restriction factor as has been explained by (E. R. Lemon, et. al., 1957). Moreover, the extent of vegetation cover and the type of vegetation in a given area influence ET by controlling levels of transpiration rates. There are differences in the process of plant metabolism, the phases of development, and the techniques of cultivating plants, all of which affect ET; as pointed by (Xueyi Yang, et. al., 2023)

On the same note, plant characteristics act as biological determinants of ET differing from biochemical factors in this case. (Hui-min Lei, et. al, 2018) opine that the type and process of plants influences the ET rates in different ways such as variation on leaf shape, root systems in addition to stomatal control mechanisms. The second is the so-called leaf area index (LAI); plants with more extensive leaves have a larger capacity for transpiration as a larger surface that directly interacts with water vapor, according to (Yasunori Igarashi, et. al., 2015)

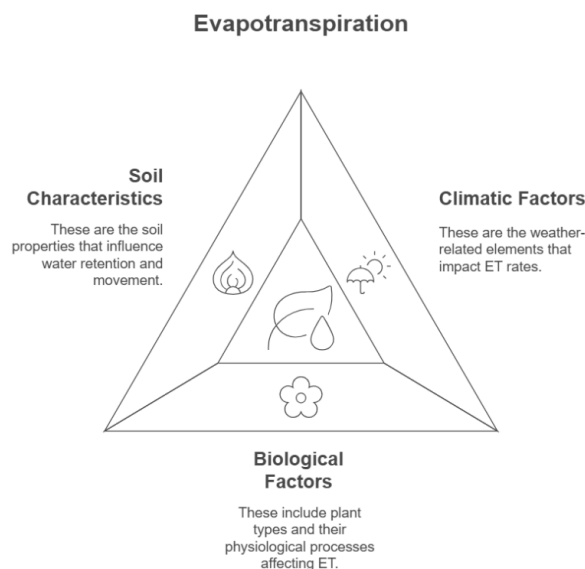


Figure 1 Main factors affect evapotranspiration

Techniques and other physical tools used to calculate evapotranspiration especially at the local or field level include 1) water balance method which involves evaluation of depletion of water in the soil, 2) the weighing lysimeter which seek to weigh water losses from the soils and plants through measuring changes in weight (William Fenner, et. al., 2019). They offer precise direct measurements though they are expensive and are difficult to fasten, 3) PM equation, 4) Bowen ratio energy balance which helps estimate ET using the measurements of different temperature and humidity rates, mainly where the climate is wet (D.E. Angus, el. at., 1984). However, Bowen ratio is useful in the open field study, while its measures can be slightly off in very dry and windy conditions., 5) Eddy covariance which directly measures water vapor and heat fluxes in the atmosphere using instance sensors and is applicable with large, uniform areas like forests and crop fields. It is a preferred micrometeorological method for continuous ET data collection, though it requires complex setup and calibration and large aperture reflection. However, these approaches are mostly nuanced, costly and used often in spatial domain, and are, therefore, most useful in the academic/research paradigms. While scaling up production of these

types of equipment remains an expensive proposition. At the larger scales from the irrigation scheme level up to water sheds and regional or even national scales, the options for measurement of actual evapotranspiration at present are for satellite remote sensing (RS). Figure 2 display the dominant techniques to estimate evapotranspiration

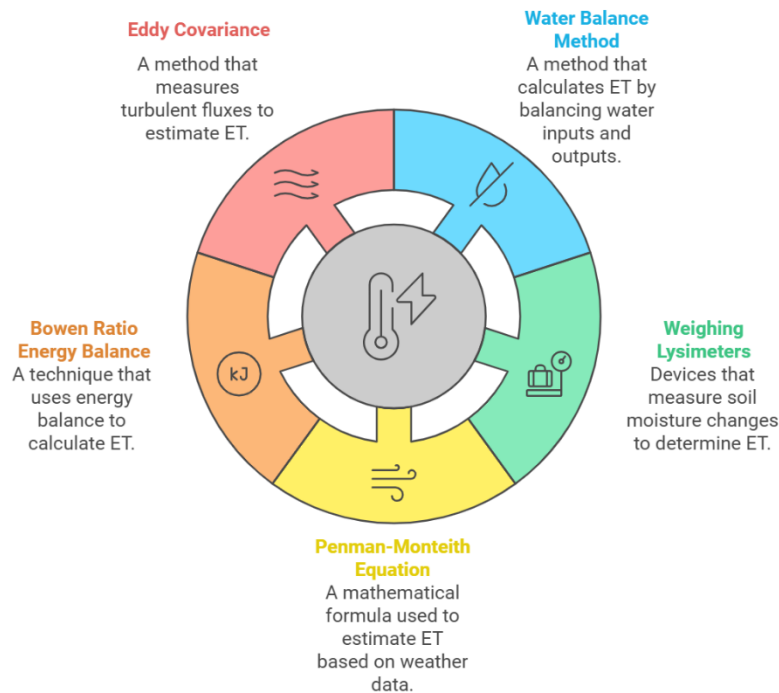


Figure 2 Techniques for Evapotranspiration Estimation

II. Methods and Data

2.1 Study areas description

The Delta region in Egypt is one of the oldest agricultural areas worldwide where the ancient Egyptians built the oldest civilization. The Delta region covers around 22,000 Km² **Error! Reference source not found.** and is considered as the most fertilized are in Egypt due to annual floods before High Aswan Dam's construction and operation in mid of the 19th century.

This area used to use flood irrigation from early ages and still use these irrigation techniques to overcome increasing salinity and soil deterioration in this region. The Nile Delta is characterized as hyper-arid climate except the northern part, which is considered semi-arid with average rainfall of 200mm in the winter season. (Omar, Mohie et al., 2019). Accordingly, the huge area of the delta region consumes a huge amount in the evapotranspiration process. Optimum utilization of available water resources in this region requires extensive study for evapotranspiration. As it's acknowledged, the evapotranspiration process occurs due to interaction between soil, water bodies, and plant based on attached metrological conditions. Evapotranspiration is one of the important surface land fluxes, which associates the process of evaporation from the soil, evaporation from water bodies, and that of transpiration from plants, re-counting the transformation of water vapour from the land to the atmosphere. Accurately estimating evapotranspiration in agricultural systems is of extremely difficult and high importance for efficient use of water resources and detailed irrigation scheduling operations. (I. Ghat et al., 2021). Evapotranspiration modelling is a complex process and requires field measurements for calibration and validation stages. Fortunately, the Delta region hosts two mega research stations; one belongs to the ministry of water resources and irrigation and the other one belongs to ministry of agriculture and land reclamation.

- Sakha study area

Sakha research station is located in Kafr ElShiekh governorate in the centre of Delta region. It belongs to the Agriculture Research Centre (ARC), Ministry of Agriculture and Land Reclamation (MoALR). The station is located at (31.094059 N, 30.933899 E)

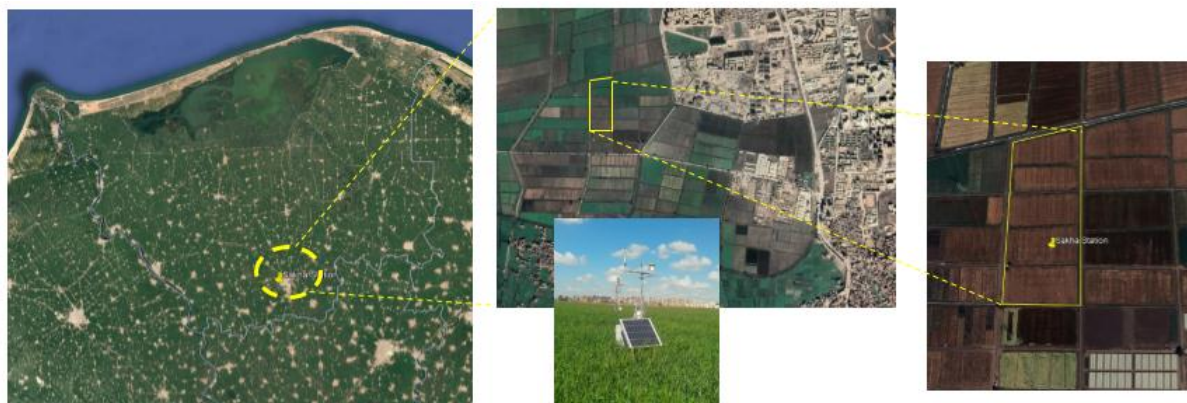


Figure 3 Sakha station, ARC, MoALR, Egypt

The station hosts the most popular devices used to measure and estimate evapotranspiration with different approaches; eddy covariance that has been developed based on continuous determination of the carbon and water vapor flows of an ecosystem, and CORDOVA station that has been developed based on Surface Energy Balance (SEB) approach as well as Surface Energy Balance (SEB) tower which has been used in this paper

2.2 Evapotranspiration Remote sensing datasets

Remote sensing datasets provide opportunities in terms of efficiency as well as scalability for ET estimates over different temporal and spatial scales. These datasets retrieve ET by incorporating surface energy balance models and vegetation index forage from spectral data in satellite observations. MODIS, and WaPOR are some of the well-known open-source datasets that can be used to estimate ET.

2.2.1 ET MODIS16A2 Dataset

MOD16A2 is an 8-day average global product derived from the MODIS which estimates terrestrial evapotranspiration and potential evapotranspiration at 500 meters spatial resolution. It turns out that this product is significant in hydrology, climate research, and water/resources management because it provides essential information on the water exchange between the land surface and the atmosphere. MOD16A2 ET data encompasses actual evapotranspiration, including both soil evaporation and plant transpiration, as well as potential ET estimates. It is derived from the MODIS sensors on NASA's Terra and Aqua satellites, covering all vegetated land areas globally.

MOD16A2 is globally available every 8 days and provides ; Evapotranspiration (ET) “Total water vapor fluxes to the atmosphere, integrating evaporation and transpiration from vegetation and bare soil”, Potential Evapotranspiration (PET)” Maximum ET under idealized conditions of sufficient water availability”, and 8-Day Composite Data” The data is averaged over 8-day periods to mitigate issues related to cloud cover and noise, providing consistent temporal snapshots”.

The MOD16A2 algorithm integrates various remote sensing inputs with meteorological data to calculate ET and PET, as described below in Figure 4. Penman-Monteith equation (PM) is the reference to generating MOD16A2 ET data relies. PM is a widely accepted method for calculating ET based on surface energy balance principles. The MOD16A2 product is widely used for applications requiring an understanding of water availability, agricultural productivity, and ecosystem health, as it provides a reliable ET estimate that is spatially continuous and temporally average

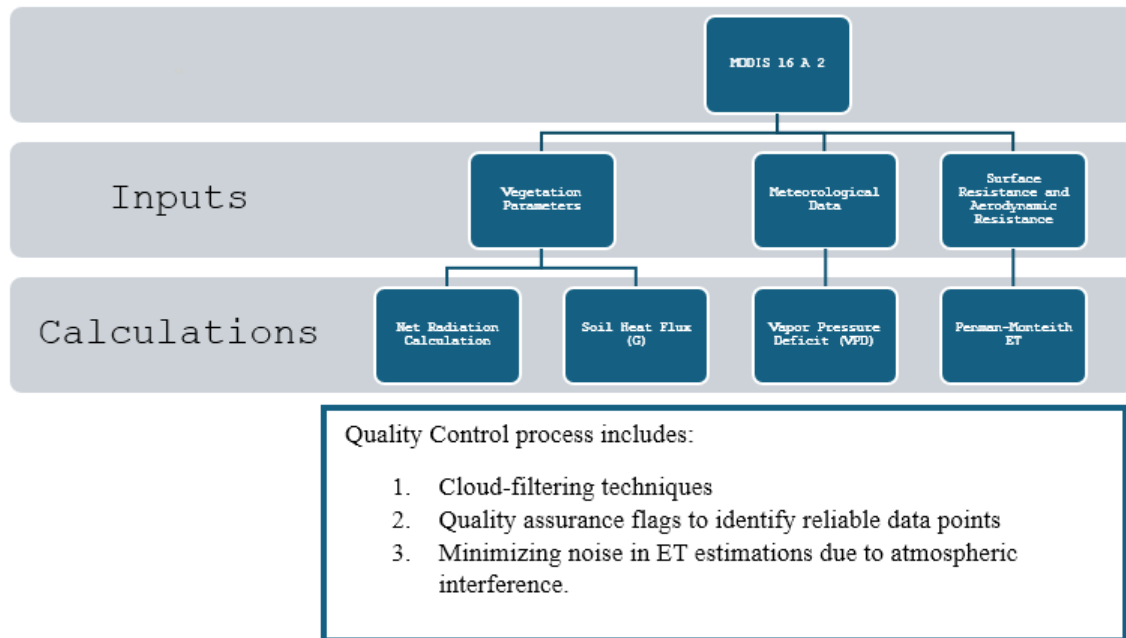


Figure 4 Schematic diagram shows the calculation and inputs to estimate MODIS16A2 Evapotranspiration data

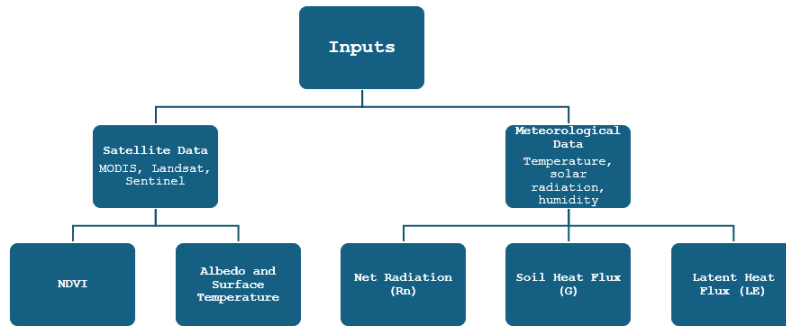
2.2.2 WaPOR Data

WaPOR (Water Productivity Open access of Remote sensing data) is the FAO's portal designed to help countries monitor water productivity, identify productivity gaps, and suggest strategies to bridge these gaps. This platform is the result of a project funded by the Ministry of Foreign Affairs of the Kingdom of the Netherlands. WaPOR provides detailed ET, precipitation, and biomass production data, helping to analyze water productivity on a pixel-by-pixel basis. It is particularly valuable for tracking water use in agriculture, supporting sustainable agricultural practices by enabling countries to monitor, analyze, and improve crop water productivity. (FAO, WaPOR - portal, 2023.). WaPOR is available at different spatial (250 m, 100 m, and 30 m) and temporal (daily, monthly, and yearly) resolutions, tailored to different agricultural and hydrological applications. WAPOR data can be used for Assessing water productivity and efficiency in agriculture, supporting irrigation planning and drought response strategies, providing actionable data for policymakers and farmers to optimize water use.

The WaPOR algorithm is based on the FAO's Surface Energy Balance Algorithm for Land (SEBAL) and adaptations of the ETLook model, which is a two-source energy balance approach for estimating ET and requires land surface temperature, vegetation indices, and meteorological data from satellites. ET Look is most useful since it operates under a range of atmospheres, including cloudy conditions, against which other models such as METRIC are confined to (Mostafa Javadian, et. al., 2019). The key processes in the WaPOR algorithm involve the following steps as shown in The algorithm *separates transpiration from vegetation and evaporation from soil using inputs from NDVI, soil moisture, and thermal bands to calculate Daily and Monthly ET is estimated by aggregating instantaneous ET values over time, accounting for daily variations in weather and vegetation growth.*

Then calculate Biomass Production by integrating ET with crop coefficient data, estimating how efficiently crops use water for growth, and Water Productivity by relating biomass to ET, providing metrics on water use efficiency across various agricultural areas.

Figure 5



The algorithm separates transpiration from vegetation and evaporation from soil using inputs from NDVI, soil moisture, and thermal bands to calculate Daily and Monthly ET is estimated by aggregating instantaneous ET values over time, accounting for daily variations in weather and vegetation growth.

Then calculate Biomass Production by integrating ET with crop coefficient data, estimating how efficiently crops use water for growth, and Water Productivity by relating biomass to ET, providing metrics on water use efficiency across various agricultural areas.

Figure 5 Schematic diagram shows the calculation and inputs to estimate WaPOR Evapotranspiration data

2.3 In-Situ Data

Actual evapotranspiration data was collected over five agriculture seasons at Sakha research station, part of Agriculture Research Center (ARC). Among different instruments, Energy Balance (EB) flux tower has been installed and equipped with a range of meteorological instruments designed to measure various components of the surface energy balance (EB). Sensible heat flux (H) was calculated using high-frequency data collected by a datalogger. Low-frequency measurements of net solar radiation and soil heat flux were utilized to determine the 30-minute averages of net radiation (Rn) and soil heat flux (G). Additional measurements of soil temperature gradient and soil moisture enabled the calculation of heat storage (S) within the soil surface layer. The collected data from EB sensors have been illustrated in Figure 6. Table 1 lists each dataset’s season, the cultivated crop, cultivation start date, and harvesting date. *Wheat* is the dominant winter crop in this region, showing recorded minimum actual evapotranspiration values of 0.3, 0.5, and 0.02mm, with maximum values reaching 4.7, 4.3, and 6.5 mm for the winter of 2020, 2021, and 2022 respectively. The dataset includes 152 records for winter 2020, 157 for 2021, and 162 for 2022. For the summer season, data was collected for maize in 2020, with minimum and maximum actual evapotranspiration values of 1.1 mm and 5.8 mm, respectively, and for rice in 2021, with a minimum of 2 mm and a maximum of 5.9 mm. Figure 6, illustrates the five seasons of actual evapotranspiration data.

Table 1 Attribute of each agriculture season

Season	Cultivated Crop	Strat Date	End Date
Winter 2019-2020	Wheat	1 Dec 2019	30 April 2020
Summer 2020	Maize	20 July 2020	31 Oct 2020
Winter 2020-2021	Wheat	25 Nov. 2020	30 April 2021
Summer 2021	Rice	16 June 2021	31 Oct. 2021
Winter 2021-2022	Wheat	5 Dec. 2021	15 May. 2022

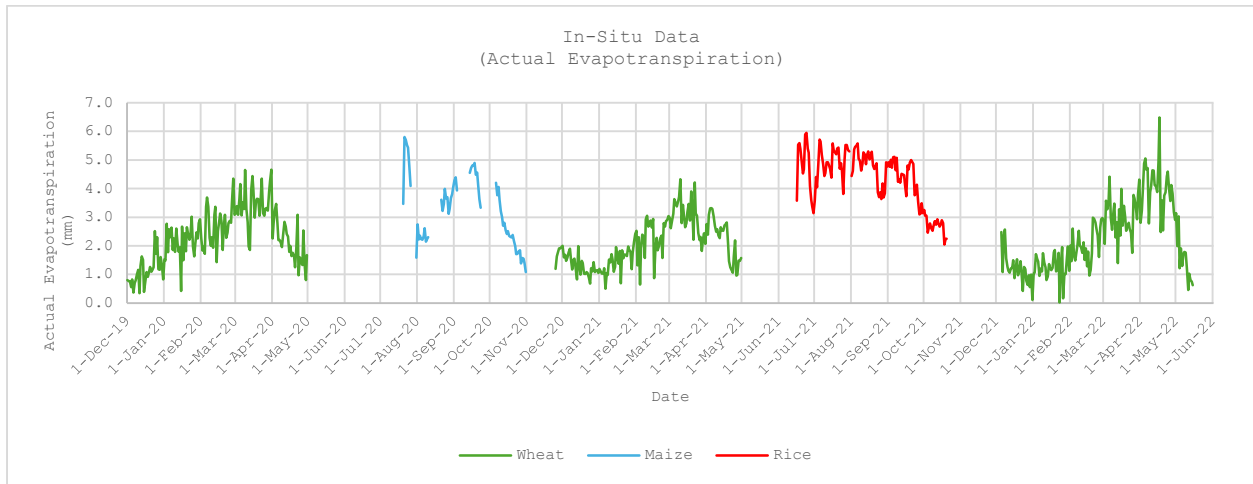


Figure 6 in-situ actual evaporation along five agriculture seasons from winter 2019/20 to summer 2020

2.4 Performance indicators criterions used to assess ET product “MODIS16A2 and WaPOR data”
 Eight statistical indicators have been used to assess remotely sensed ET data reference to ET measurements. Table 2 illustrate each factor with definition, formula, ideal value, and interpretation of the values

Table 2 List of statistical indicators with attached definition, formula, ideal values, and interpretation of the values

Indicator	Definition	Formula	Ideal value	Interpretation
R² (Coefficient of Determination)	Calculates the extent to which attributes and features in observed data are accounted for by the model	$R^2 = 1 - \frac{\sum_{i=1}^n (O_i - P_i)^2}{\sum_{i=1}^n (O_i - \bar{O})^2}$ O _i : Observed value P _i : Predicted value Ō: Mean of observed values n: Number of observations	1	<ul style="list-style-type: none"> • 0.8 - 1: Excellent fit • 0.5 - 0.8: Moderate fit • <0.5: Poor fit
Correlation Coefficient	Strength and direction of linear relationship between observed and predicted ET	$r = \frac{\sum_{i=1}^n (O_i - \bar{O})(P_i - \bar{P})}{\sqrt{\sum_{i=1}^n (O_i - \bar{O})^2 \sum_{i=1}^n (P_i - \bar{P})^2}}$ O _i : Observed value P _i : Predicted value Ō: Mean of observed values n: Number of observations P̄: Mean of predicted values	1 or -1	<ul style="list-style-type: none"> • 0.8 - 1: Strong correlation • 0.5 - 0.8: Moderate positive correlation • 0 - 0.5: Weak correlation • Negative values: Inverse relationship
RMSE (Root Mean Square Error)	Average magnitude of errors between observed and predicted ET values (in same units as ET)	$RMSE = \sqrt{\frac{1}{n} \sum_{i=1}^n (O_i - P_i)^2}$	0	Higher accuracy is represented by values below; lows of RMSE may differ depending on the application but denote better performance of a dataset.
Relative RMSE (rRMSE, %)	The percentage of the mean observed ET	$rRMSE = \left(\frac{RMSE}{\bar{O}} \right) * 100$	0%	<ul style="list-style-type: none"> • <10%: Very good • 10% - 20%: Acceptable • >20%: Poor accuracy
MBE (Mean Bias Error)	average bias (systematic error) in predicted ET values	$MBE = \frac{1}{n} \sum_{i=1}^n (P_i - O_i)$	0	<ul style="list-style-type: none"> • The positive values, these values would mean overestimation. • The negative values mean that there is actually an underestimation. • The absolutes close to zero are preferable.
PB (Percentage Bias)	percentage of observed ET	$PB = \left(\frac{\sum_{i=1}^n (P_i - O_i)}{\sum_{i=1}^n O_i} \right) * 100$	0%	<ul style="list-style-type: none"> • <10%: Very good • 10% - 20%: Acceptable • >20%: Poor accuracy
EFF (Efficiency)	predictive ability of the model relative to the mean observed ET	$EFF = 1 - \frac{\sum_{i=1}^n (O_i - P_i)^2}{\sum_{i=1}^n (O_i - \bar{O})^2}$	1	<ul style="list-style-type: none"> • >0.5: Good model performance • 0 - 0.5: Moderate performance • <0: Poor performance (model performs worse than mean)

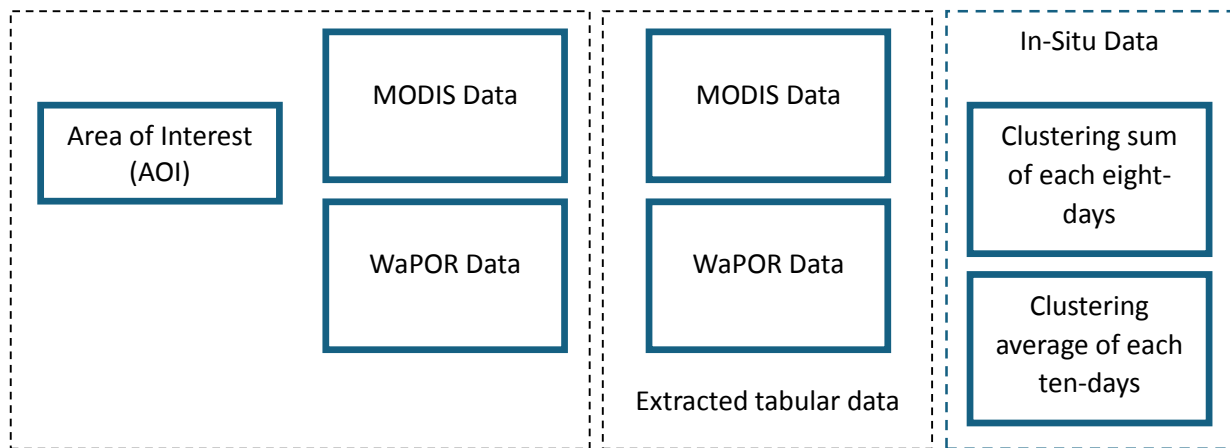
KGE (Kling-Gupta Efficiency)	Balances correlation, bias, and variability for overall performance	$KGE = 1$	1	0.75 - 1: Very good 0.5 - 0.75: Acceptable <0.5: Poor performance
		$-\sqrt{(r-1)^2 + \left(\frac{\sigma^P}{\sigma^O} - 1\right)^2 + \left(\frac{\bar{P}}{\bar{O}} - 1\right)^2}$		

III. Result, analysis and discussions

3.1 Data analysis

In the MODIS16A2 dataset, pixel values in the Evapotranspiration (ET) layer represent cumulative evapotranspiration for each eight-day composite period (NASA, 2013). To align with this, the measured data was clustered into eight-day groups, and the total for each period was calculated for comparison. Similarly, WaPOR data provides pixel values representing a 10-day average. To facilitate comparison with ground measurements, a pre-analysis was conducted to calculate the sum over eight days for MODIS data and the 10-day average for WaPOR data, matching each dataset’s respective time intervals. Available dates from the MODIS and WaPOR datasets were extracted in Google Earth Engine (GEE) for the specified area of interest.

3.1.1 MODIS16A2 vs In-Situ Data Winter 2019/2020 – Wheat



For MODIS16A2 data and in-situ data in winter 2019/2020, the results show similar trend except 1st Jan’s record which is almost identical between two datasets as shown in Figure 7. MODIS16A2 data shows a relatively lower spread of values with a median around 10 and an upper whisker around 20 and In-Situ data has a wider spread, with values reaching up to around 30, indicating higher variability as shown in Figure 8.

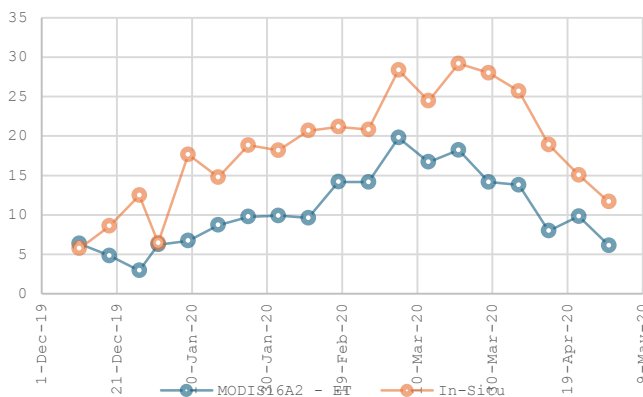


Figure 7 Comparison between MODIS16A2 - ET data and In-Situ data for winter2019/2020 cultivated with Wheat

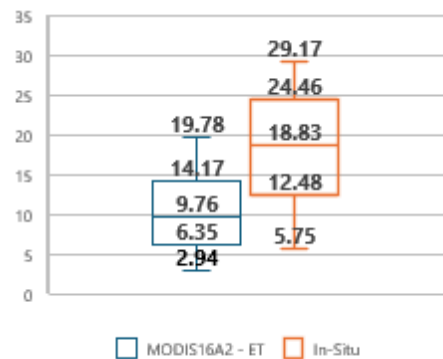


Figure 8 box plot compares the distribution of MODIS16A2 - ET and In-Situ data for winter2019/2020 cultivated with Wheat

Winter 2020/2021 - Wheat

The trend analysis for MODIS16A2 and In-Situ data from December 2020 to May 2021 shows their variation over time. Figure 9 shows the fluctuations in both datasets, with In-Situ values generally being higher than MODIS16A2 during this period. The analysis shows an increase in both datasets transitioning from winter to spring, with a more significant rise in In-Situ values.

Figure 10, This box plot reinforces the insight that In-Situ measurements generally show higher ET values with greater variability compared to MODIS-derived ET values. Both datasets show an upward trend from December to March, with MODIS16A2 data gradually rising, while In-Situ data shows a steeper increase, peaking in March. In-Situ reaches its highest average ET value in March 2021, indicating higher evapotranspiration during this period. MODIS16A2 also peaks around March but with a lower maximum. Both datasets show a decline from March through May, with In-Situ values dropping more sharply than MODIS16A2.

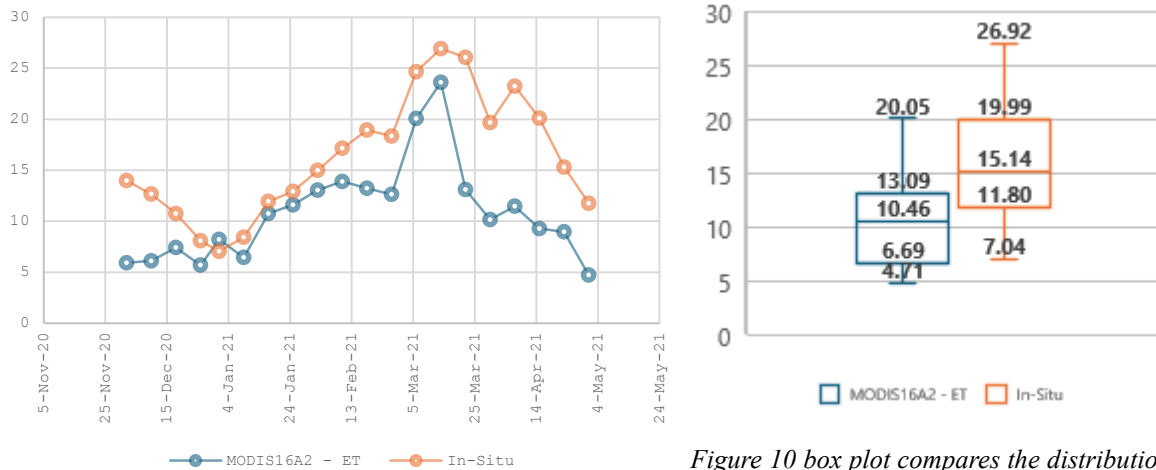


Figure 9 Comparison between MODIS16A2 - ET data and In-Situ data for winter2020/2021 cultivated with Wheat

Figure 10 box plot compares the distribution of MODIS16A2 - ET and In-Situ data for winter2020/2021 cultivated with Wheat

Summer 2021 - Rice

The trend analysis for MODIS16A2 and In-Situ data from December 2020 to October 2021 as shown in Figure 11 reveals that; Both date sets have a high value in March but more significantly, the In-Situ data are much higher than the MODIS16A2 data at the same time period. As exhibited in the graph below, both In-Situ and MODIS16A2 dataset drop to their lowest in early summer, In-Situ spikes in August before a sharp decline. Meanwhile, In-Situ ET values are considerably variable, especially revealing another spike in June followed by the least increase in October. All in all MODIS16A2 values are usually lower than In-Situ. From this seasonal comparison it can be inferred that while In-Situ measures may be capturing more unique or localized peaks or dips in ET, MODIS is substantially underestimated.

Figure 12 compares the distribution of MODIS16A2 - ET and In-Situ data, showing distinct characteristics for each dataset. The Central Tendency for MODIS16A2 - ET has a slightly higher median value, equal to 7.66, as opposed to a higher median value obtained for In-Situ equal to 36.51, so In-Situ appears to use much higher ET values for calculations. Regarding to the Interquartile Range (IQR): Nevertheless, MODIS16A2 has a higher contrast range and lower variability, with an IQR of about 5.94 to 9.90. Similar to the In-Situ data has a much wider IQR ranging from roughly 28.85 to 40.19, indicating far greater spread of ET measurements. For Range and Outliers; The minimum and maximum values are 5.94 and 12.71 respectively for MODIS16A2 having no significant outliers. Using In-Situ data it varies from 18.67 to 42.04, suggesting great variability which suggest periodic reading or more frequent fluctuation or there could be outlier. In general, The results show that , In-Situ measurements give higher and highly skewed ET values than MODIS16A2 which could be attributed to cultivating Rice which influences the In-Situ data or remotely sensed data.

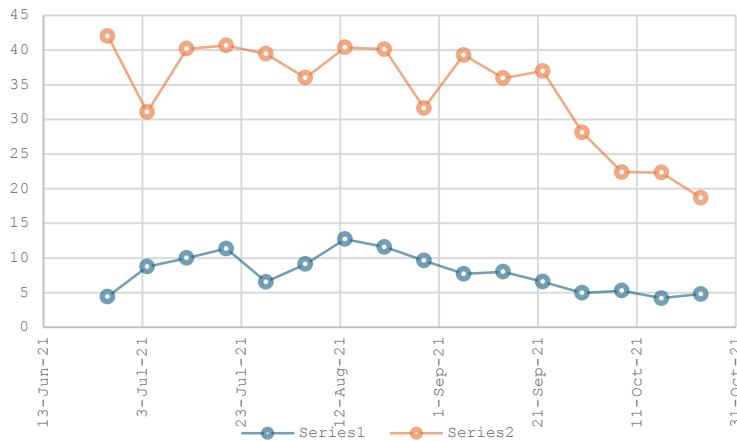


Figure 11 Comparison between MODIS16A2 - ET data and In-Situ data for summer 2021 cultivated with Rice

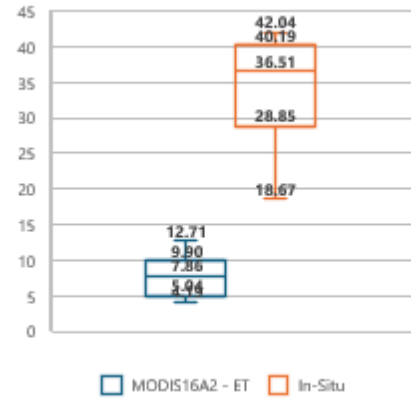


Figure 12 box plot compares the distribution of MODIS16A2 - ET and In-Situ data for summer 2021 cultivated with Rice

Winter 2021/2022 – Wheat

The trend analysis from 11th December 2020 to 17th May 2022 reveals that it has been observed that, In-Situ systematically reports higher ET values and higher degree of variability across the scale of seasons; compared to MODIS16A2 range that appears to be comparatively flat. This trend analysis also shows the difference in MODIS16A2 and In-Situ, the latter capturing relatively bigger oscillations in the seasonality as shown in Figure 13.

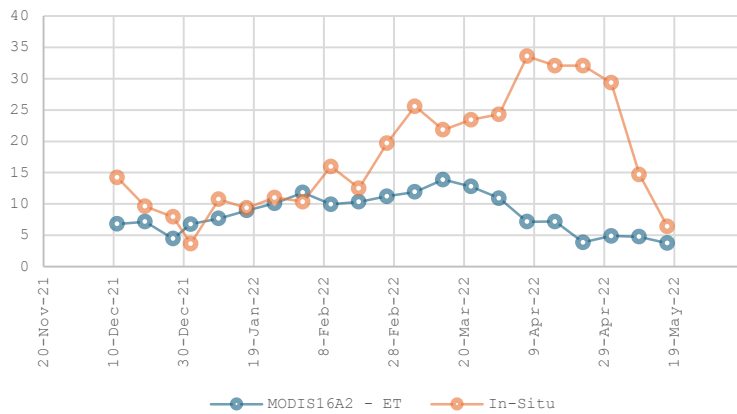


Figure 13 Comparison between MODIS16A2 data and in-situ data for winter 2021/2022 cultivated with Wheat

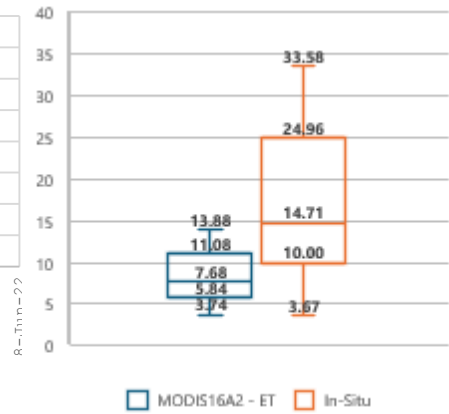


Figure 14 box plot compares the distribution of MODIS16A2 - ET and In-Situ data for winter 2021/2022 cultivated with Wheat

3.1.2 WaPOR vs In-Situ Data

Winter 2019/2020 - Wheat

WaPOR data starts from 11 December 2019, which begins at 0.4 and ranges up to 4.3 on 21 March 2020 and declines to 1.8 on 01 May 2020. MODIS data starts at 0.77, follows an almost similar pattern to the above calculation rising to a peak of 3.63 on April 1, 2020, before dropping to 1.67 on May 1, 2020 as illustrated in Figure 15. As illustrated in the Box and Whisker plot in Figure 16, both medians represent similar values although the median of in-situ data was slightly higher than the recorded via WaPOR data. We can reason that WaPOR data should have a larger spread measured data has less variation about the median samples.

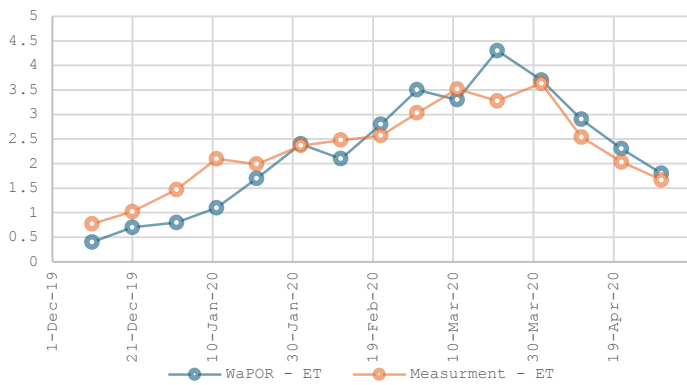


Figure 15 Comparison between WaPOR v03 data and in-situ data for winter 2019/2020 cultivated with Wheat

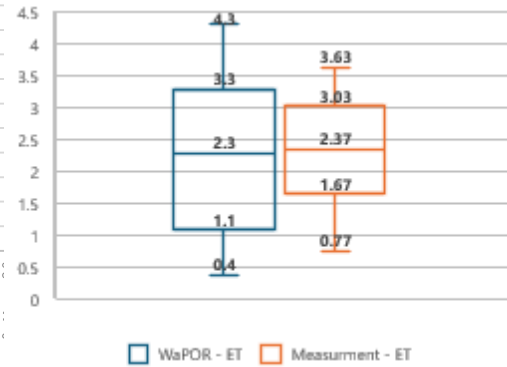


Figure 16 box plot compares the distribution of WaPOR v03 - ET and In-Situ data for winter 2019/2020 cultivated with Wheat

Summer 2020 – Maize

Figure 17 illustrates that MODIS16A2 and In-Situ ET values from July to October 2020 shows the following; The cases in two datasets are increasing from July to mid-September and gradually decrease to early September and after. Both values reduce from late September through October but MODIS16A2 has a bit higher values than In-Situ at the last Value, MODIS16A2 datasets are lower than In-Situ at the initial point of measurement in the year starting from July, after some days of measurements, MODIS16A2 values are higher than In-Situ at early August and continue to be so until October. The variability of change of In-Situ measurements is also higher compared to In-Situ-R measurements during August 1st and October 1st, MODIS16A2 reaches it highest with a value of 4.8 in early September while In-Situ has its highest value of approximately 4.1 at the same time. The trough in October is deeper in In-Situ at 1.65, while in MODIS16A2, the value is at 2.6. This plot suggests that there is some differences in the variability as well as the relative scale in the two datasets, especially with the onset of different seasons.

Figure 18, for the box plot shows that the result of the comparison of the WAPOR - ET and Measurement - ET. Here's a breakdown of the key insights as ; WAPOR specific to ET has a median of about 3.85 whereas the median for Measurement specific to ET is slightly lower at 3.65. This means that in general the WAPOR data contains slightly higher ET values than the corresponding measurement data. WAPOR - ET has a range which is around 2.43 and 4.73 and the IQR is moderate. Measurement, it is noticeable that ET has an IQR of 2.33 to 4.04 thus has slightly less variability than WAPOR but with a slightly larger range. It has values ranging from 1.80 in the smallest value recorded to 5.10 in the largest value recorded. Measurement ET has a narrower range of averaged scores with a range of 1.66 to 4.69 revealed that there were not many extreme scores present among the respondents.

On balance, the WAPOR data once again appears somewhat more dispersed and variable and the Measurement data more centralized. This pattern might mean that there is wider variation of ET values under the AEP by WAPOR that may be attributed to differences in data collection or estimation.

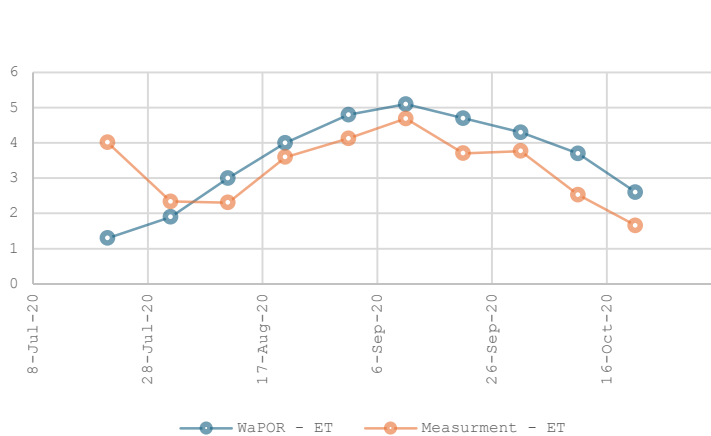


Figure 17 Comparison between MODIS16A2 data and in-situ data for summer 2020 cultivated with Maize

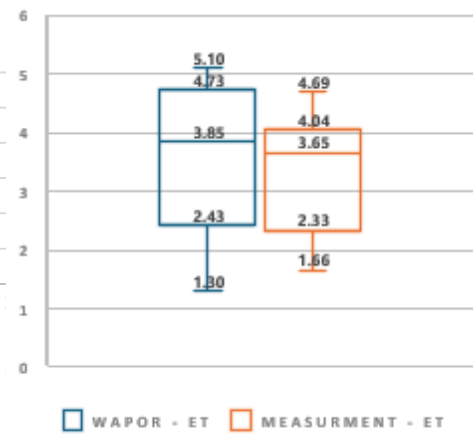


Figure 18 box plot compares the distribution of WaPOR v03 - ET and In-Situ data for summer 2020 cultivated with Maize

Winter 2020/2021 – Wheat

As it is clear from Figure 20 WaPOR - ET data displays a broader range and higher variability, while Measurement - ET data remains more consistent around its median. This difference might be due to WaPOR’s methodology capturing a broader spectrum of ET values

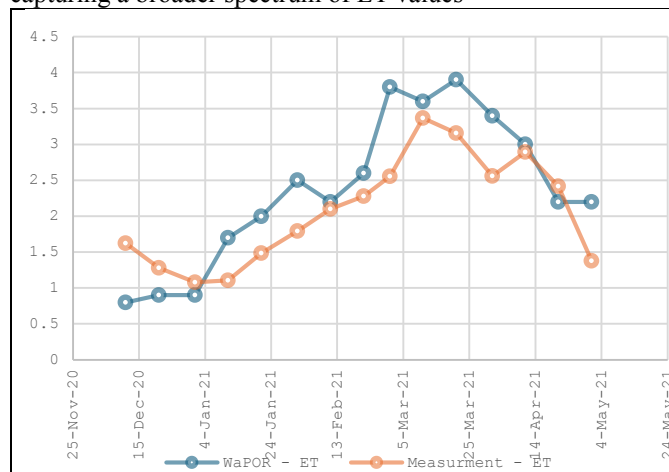


Figure 19 Comparison between MODIS16A2 data and in-situ data for winter 2020/2021 cultivated with Wheat

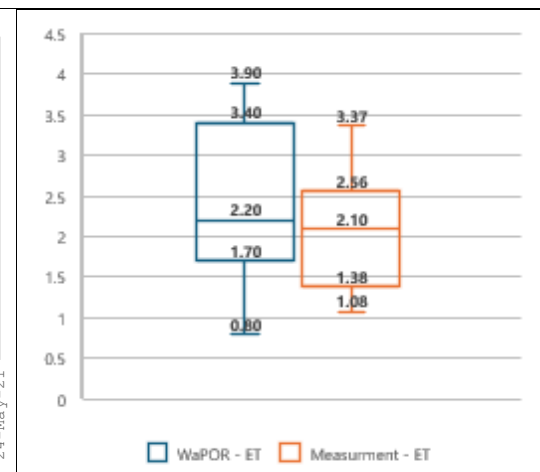


Figure 20 box plot compares the distribution of WaPOR v03 - ET and In-Situ data for winter 2020/2021 cultivated with Wheat

Summer 2021 – Rice

The comparison of WaPOR and In-Situ ET values from July to October 2021 Figure 21 reveals that; Both sets show an increase through July and August and reached their highest point in early September. Such a rise corresponds to the normal higher ET in summer period that is evident from the observations made in this study. After reaching the highest value in early September, both values decreases constantly up to the end of October. Both In-Situ and WaPOR - ET show an increase, but the In-Situ values are generally greater than WaPOR - ET with a maximum value reaching about 4.0 in the month of August as compared to WaPOR - ET with a definite maximum of about 5.07 in the month of August as compared to WaPOR - ET with a gradual rise and fall as compared to the In-Situ values that have sharp rise and fall. There is a drop off from mid September to late October, and In-Situ ends at a lower of around 2.61 and WaPOR - ET at approximately 2.6. This pattern demonstrates the seasonality of either In-Situ is obtaining relatively higher ET values than the WaPOR - ET derived data due to some micro climatic factors.

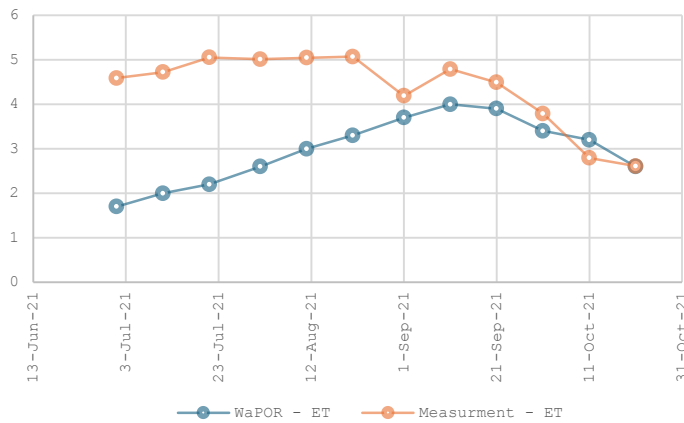


Figure 21 Comparison between MODIS16A2 data and in-situ data for summer 2021 cultivated with Rice

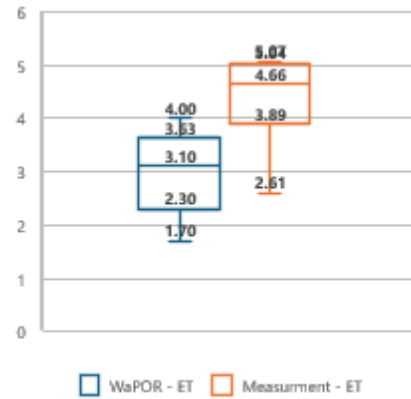


Figure 22 box plot compares the distribution of WaPOR v03 - ET and In-Situ data for summer 2021 cultivated with Rice

Winter 2021/2022- Wheat

Figure 23 illustrates the comparison of WaPOR and In-Situ ET values from December 2021 to May 2022 shows that; Trend Alignment: Both datasets follow an upward trend from December through early April, peaking in early April for WaPOR and slightly later for In-Situ. After reaching their peaks, both datasets display a decline through April and May. Magnitude Differences: WaPOR values generally remain higher than In-Situ throughout this period, especially in March and April, where WaPOR reaches a maximum around 5.7. In-Situ shows a more gradual increase, peaking at a lower value of about 4.14 in April. For Variability, WaPOR exhibits a steeper increase and decrease, indicating more sensitivity to seasonal changes during the period. In-Situ values are smoother and less variable, reflecting a more gradual response to environmental changes. This analysis suggests that WaPOR captures more dynamic changes in ET, while In-Situ measurements show more stable, less extreme values

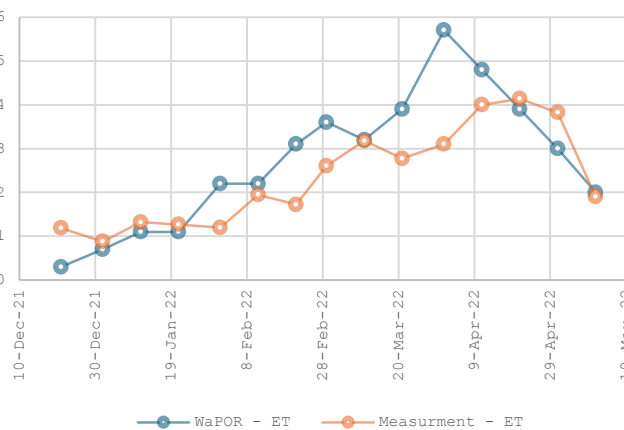


Figure 23 Comparison between MODIS16A2 data and in-situ data for winter 2021/2022 cultivated with Wheat

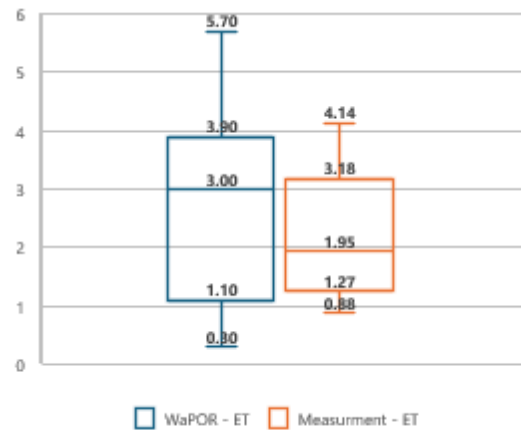


Figure 24 box plot compares the distribution of WaPOR v03 - ET and In-Situ data for winter 2021/2022 cultivated with Wheat

IV. Performance indicators for MODIS16A2 and WaPOR data

Table 3 and Figure 25 show the detailed analysis of the seasonal performance of MODIS16A2 and WaPOR across different seasons and crops

Table 4 values of statistical factors regarding MODIS16A2 and WaPOR data

Season	Winter 2019/2020 Wheat	Winter 2020/2021 Wheat	Summer 2021 Rice	Winter 2021/2022 Wheat
--------	------------------------	------------------------	------------------	------------------------

Product	MOD16A2	WaPOR	MOD16A2	WaPOR	MOD16A2	WaPOR	MOD16A2	WaPOR
R2	0.761	0.865	0.590	0.731	0.350	0.009	0.540	0.647
Correlation	0.872	0.930	0.768	0.855	0.591	-0.095	0.735	0.804
RSME (mm)	1.964	0.125	1.457	0.159	6.736	0.517	1.828	0.252
rRSME (%)	0.108	0.054	0.090	0.077	0.198	0.119	0.124	0.108
MBE(mm)	0.406	0.003	0.267	-0.021	1.640	-0.021	0.336	-0.026
PB(%)	42.320	1.918	33.024	-14.900	76.963	31.741	34.279	-16.413
EFF	-0.515	0.657	-0.104	0.340	-1.380	0.340	0.092	0.182
KGE	0.435	0.958	0.799	0.942				0.930

▪ **R² (Coefficient of Determination)**

Winter 2019/2020 - Wheat: WaPOR performs better Coefficient of Determination ($R^2=0.865, 0.865, \text{ and } 0.865$) compared to MODIS16A2 ($R^2=0.761, 0.761, \text{ and } 0.761$), which indicate that WaPOR has a better descriptive for ET variations.

Winter 2020/2021 - Wheat: WaPOR ($R^2=0.731, 0.731, \text{ and } 0.731$) again outperforms MODIS16A2 ($R^2=0.590, 0.590, \text{ and } 0.590$).

Summer 2020 - Rice: Both products have low R^2 values, with WaPOR almost negligible at 0.009, suggesting a poor fit, especially for WaPOR.

Winter 2021/2022 - Wheat: WaPOR ($R^2=0.647, 0.647, \text{ and } 0.647$) is slightly better than MODIS16A2 ($R^2=0.540, 0.540, \text{ and } 0.540$).

▪ **Correlation**

All seasons of the study indicate that WaPOR has better correlation values than MODIS16A2, with the exception of Season 4 (Rice) that has a negative correlation estimate of -0.0954.

▪ **RMSE (Root Mean Square Error)**

The evaluations show that, in terms of accuracy, RMSE for the WaPOR dataset is substantially lower than for MODIS16A2 in all the considered seasons. For instance, in the Wheat Season MODIS16A2 has an RMSE of 1.9642mm compared to RMSE of only 0.1247mm for the case of WaPOR.

▪ **Relative RMSE (rRMSE, %)**

Another proof is that compared to the parameters of other models, the relative RMSE of WaPOR is significantly lower and establish more reliable performance. For instance, the MODIS16A2 is 9.02% in Season 3 of rRMSE, whereas, the WaPOR was state 7.67%.

▪ **MBE (Mean Bias Error, mm)**

As evident from the above results, there is reduced MBE observed through out majority of the seasons with some of them close to zero implying very low bias. MODIS16A2 is again higher in biases especially for the first and fourth seasons.

▪ **PB (%)**

Smaller PB are noted on WaPOR which indicate that it captures seasonal pattern of evapotranspiration better. For example, in Season 1, MODIS16A2 has high PB of 42.32percent and low PB of WaPOR at 1.92percent.

▪ **Efficiency (EFF)**

In general, brought out that EFF values of WaPOR are higher than MODIS16A2 indicating better performance during all the seasons. Although MODIS16A2 has favorable ODR and RSRE values, there are negative EFF values of the models for Season 1, 3, and 4.

▪ **Kling-Gupta Efficiency (KGE)**

KGE scores demonstrate that WaPOR generates comparatively higher values for all seasons, possibly the highest in Season 1 at 0.9581 against MODIS16A2 at 0.4351. High KGE values can be considered indicating better correspondence in terms of correlation and at the same time, low variability and preliminary bias.

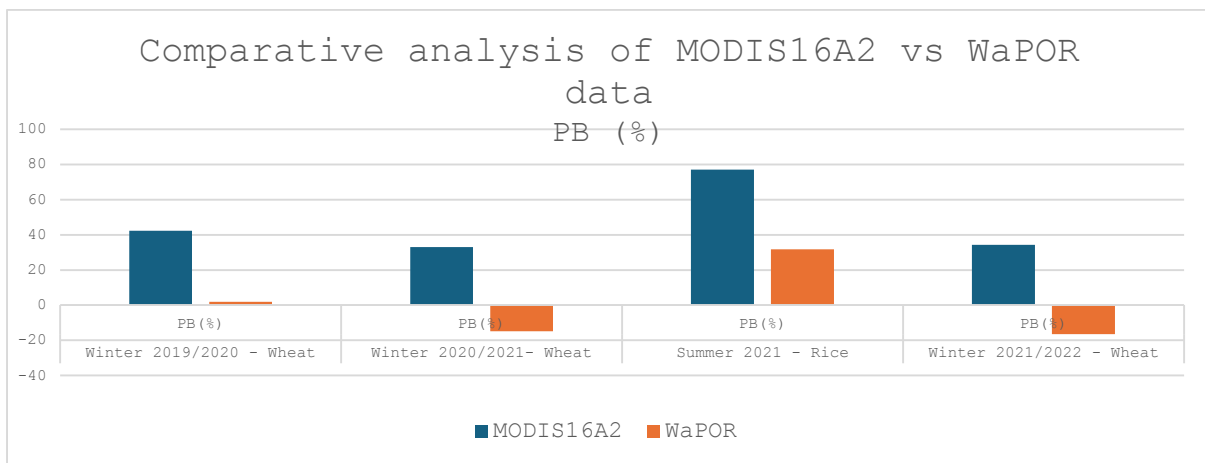
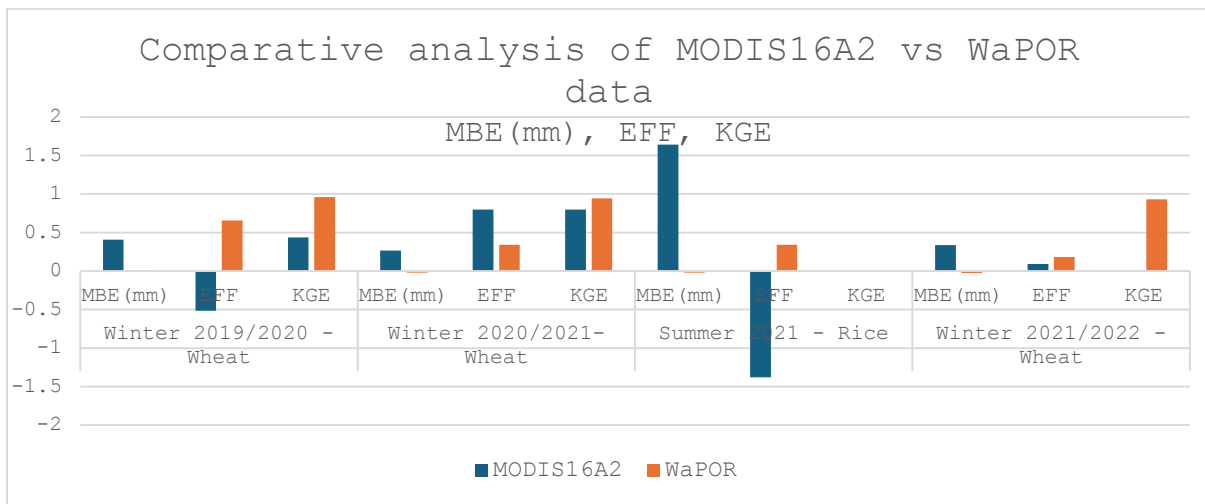
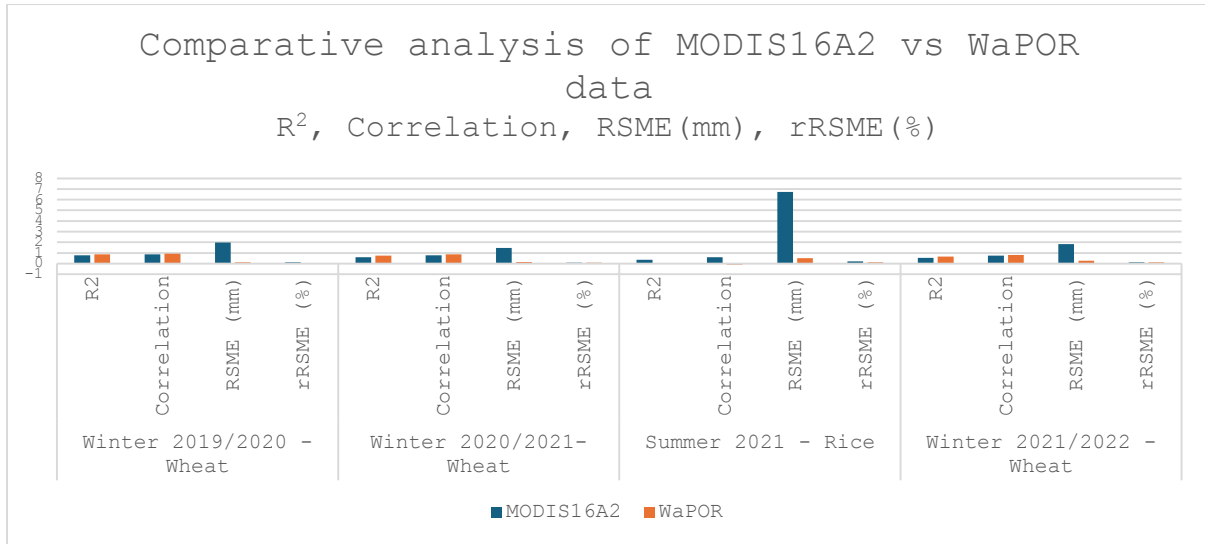


Figure 25 Comparative analysis of MODIS16A2 vs WaPOR data

V. Conclusion and Recommendations

This paper compares evapotranspiration derived from MODIS16A2 and WaPOR version 3 with the observed data. It has been realized that the accuracy of ET calculation varies greatly over different seasons of agricultural practices. On average, the results indicated that all the metrics in the present study were significantly better in WaPOR v3.0 than in MODIS16A2.

Estimated ET was expressed using four statistical parameters; R^2 (coefficient of determination), correlation coefficient, RMSE (Root Mean Square Error), and PB (Percentage Bias) to prove the higher accuracy level and closeness of the remotely sensed to the observed ET data. Specifically, the performance of WaPOR v3.0 was high in the wheat production season and its correlation and error coefficients were low. MODIS16A2, in this study, yielded higher errors and lower efficiency especially in the rice-growing seasons implying that certain crop conditions may constrain its application. Seasonal trends revealed that, during the rice growing season, both products exhibited relatively poor performance, especially MODIS16A2 which overestimated ET as indicated by high RMSE, PB, and poor efficiency values. On the other hand, during the wheat seasons both products showed better performance but with higher accuracy was achieved by WaPOR results, closer to the observed ET and with negligible amounts of bias.

For Agricultural Applications: Based on these results and the fact that WaPOR performed particularly well in wheat-growing seasons, it is suggested that the tool should be used for ET estimation in similar crops. Because it offers a high accuracy coupled with low bias, it can be used to monitor and manage water resources in agricultural status, especially where wheat or crops of similar nature are farmed.

Moreover, Integration of observed data for Calibration is very important to enhance the reliability of products incorporating the locally observed ET data for calibration will enhance model accuracy. This approach would help refine the models specific to environmental and crop conditions enhancing the possibilities for accurate water resource planning and management.

Therefore, the assessment of the present version of the WaPOR for application in agricultural ET estimates reveals significant reliability as a calculator tool for remote sensing data from different environments, especially for wheat crops. MODIS16A2 can be helpful but could need seasonal corrections or other methods for averting problems in volumetric crops such as rice. Subsequent extension with the observed data will be important toward improving the usefulness of these models in other agricultural environments.

References

- [1]. D.E. Angus, et. al. (1984). Evapotranspiration — How good is the Bowen ratio method? ELSEVIER, 133-150.
- [2]. Dunxian She, et. al. (2017). Changes in reference evapotranspiration and its driving factors in the middle reaches of Yellow River Basin, China. ELSEVIER, 1151-1162.
- [3]. E. R. Lemon, et. al. (1957). Some Aspects of the Relationship of Soil, Plant, and Meteorological Factors to Evapotranspiration. Soil Science Society of America Journal.
- [4]. FAO. (2023.). Remote sensing determination of evapotranspiration – Algorithms, strengths, weaknesses, uncertainty and best fit-for-purpose.
- [5]. FAO. (2023.). WaPOR - portal. Retrieved from WaPOR - FAO portal to monitor Water Productivity through Open access of remotely sensed derived data.: <https://www.fao.org/land-water/databases-and-software/wapor/en/>
- [6]. Huimin Lei, et. al. (2018). Biological factors dominate the interannual variability of evapotranspiration in an irrigated cropland in the North China Plain. ELSEVIR, 262-276.
- [7]. I. Ghiat et al. (2021). A Review of Evapotranspiration Measurement Models, Field Applications. Water.
- [8]. Mostafa Javadian, et. al. (2019). METRIC and WaPOR Estimates of Evapotranspiration over the Lake Urmia Basin: Comparative Analysis and Composite Assessment. MDPI.
- [9]. NASA. (2013). MODIS Global Terrestrial Evapotranspiration (ET) Product. NASA.
- [10]. Omar, Mohie et al. (2019). Estimating Actual Evapotranspiration over a Large and Complex Irrigation System of the Nile Delta in Egypt. international Journal of Recent Technology and Engineering (IJRTE), 2432-2439.
- [11]. S. Mohan, et. al. (1996). Relative importance of meteorological variables in evapotranspiration: Factor analysis approach. springer nature, 1-10.
- [12]. William Fenner, et. al. (2019). Development, calibration and validation of weighing lysimeters for measurement of evapotranspiration of crops. Revista Brasileira de Engenharia Agricola e Ambiental.
- [13]. Xueyi Yang, et. al. (2023). Response of Evapotranspiration (ET) to Climate Factors and Crop Planting Structures in the Shiyang River Basin, Northwestern China. MDPI.
- [14]. Yasunori Igarashi, et. al. (2015). Separating physical and biological controls on long-term evapotranspiration fluctuations in a tropical deciduous forest subjected to monsoonal rainfall. Advancing Earth and Space Sciences, 1262-1278.
- [15]. Ze-Xin Fan, et. al. (2013). Spatiotemporal variability of reference evapotranspiration and its contributing climatic factors in Yunnan Province, SW China, 1961–2004. Springer Nature, 309–325.